Addition of Platinum and Palladium Tri-*tert*-butyl Phosphine Groups to Open Pt−Fe and Pt−Ru Metal Carbonyl Clusters

Richard D. Adams,* Burjor Captain, Wei Fu, Jack L. Smith, Jr., and Mark D. Smith

Department of Chemistry and Biochemistry and the USC Nanocenter, University of South Carolina, Columbia, South Carolina 29208

Received October 28, 2003

Two series of new compounds, $Pt_3Fe_3(CO)_{15}[M(PBu^t_3)]$ (M = Pt, **12**; M = Pd, **14**) and $Pt_3Fe_2(CO)_{12}[M(PBu^t_3)]_2$ (M = Pt, **13**; M = Pd, **15**), were synthesized from the reactions of $Pt(PBu^t_3)_2$ and $Pd(PBu^t_3)_2$ with $Pt_3Fe_3(CO)_{15}$, **9**. All new compounds were characterized crystallographically. Compounds **12** and **14** are structurally similar and contain a $M(PBu^t_3)$ group bridging a triangular Pt_2Fe group of the starting complex **9**. These compounds can be viewed as adducts of **9** because there was no loss of carbonyl ligands during the course of the addition reaction. Compounds **13** and **15** are also structurally similar and contain two mutually bonded $M(PBu^t_3)$ groups. These metal atoms are part of a Pt_2M_2 tetrahedron that also contains an edge-bridging platinum atom and two $Fe(CO)_4$ groups that bridge the Pt−Pt bonds to this edge-bridging platinum. These compounds can be formed from **12** and **14** by replacement of one $Fe(CO)_3$ group with a $M(PBu^t_3)$ group. The M−M bond is stabilized by a bridging carbonyl ligand. The reaction of $Pt(PBu^t_3)_2$ with $Pt_2Ru_4(CO)_{18}$, **11**, afforded the complex $Pt_2Ru_4(CO)_{17}[Pt(PBu^t_3)]$, **16**. Compound **16** contains an $M(PBu^t_3)$ group that has formed a quadruple bridge across a Ru_2Pt_2 butterfly of the parent cluster **11**.

Introduction

Bimetallic catalysts containing platinum are widely used in the petroleum industry.[1] Recently, bimetallic cluster complexes have been shown to be good precursors for bimetallic nanoparticles that serve as highly active and selective heterogeneous catalysts for hydrogenation reactions.[2] Improved activity and selectivity, observed in some cases, has been attributed to synergy between the different elements.[3]

Methods for synthesizing bi- and multimetallic cluster complexes have improved significantly in recent years.[4] Recently, we have shown that metal cluster complexes readily react with the compounds $M(PBu^t_3)_2$, M = Pt or Pd, by adding $M(PBu^t_3)$ groups across metal−metal bonds.[5−7] For example, the ruthenium carbonyl cluster complexes $Ru_3(CO)_{12}$ and $Ru_6(CO)_{17}(\mu_6\text{-C})$ react with $Pd(PBu^t_3)_2$ to yield the adducts $Ru_3(CO)_{12}[Pd(PBu^t_3)]_3$, **1**, and $Ru_6(CO)_{17}(\mu_6\text{-C})[Pd(PBu^t_3)]_2$, **2**, respectively.[5] The reaction of $Ru_5(CO)_{15}(\mu_5\text{-C})$ with $Pd(PBu^t_3)_2$ and $Pt(PBu^t_3)_2$ yields the adducts $Ru_5(CO)_{15}(\mu_6\text{-C})[Pd(PBu^t_3)]$, **3** (M = Pd or Pt), which exist as isomers with open and closed metal clusters, **3a** and **3b**, and the complex $Ru_5(CO)_{15}(\mu_6\text{-C})[Pd(PBu^t_3)]_2$, **4**.[6] The $M(PBu^t_3)$ group can also add across a hetero metal−metal bond in the mixed metal cluster $PtRu_5(CO)_{16}(\mu_6\text{-C})$ to afford the adducts $PtRu_5(CO)_{16}(\mu_6\text{-C})[M(PBu^t_3)]_n$, **5** and **6**, where M = Pt and $n = 1$ or $n = 2$, respectively, and **7** and **8**, where M = Pd and $n = 1$ or $n = 2$, respectively.[7] In a previous report we described the synthesis and structure of the mixed metal "raft" cluster $Fe_3Pt_3(CO)_{15}$, **9**, as well as the compound $Pt_5Fe_2(CO)_{12}(COD)_2$, **10** (COD = 1,5-cyclooctadiene), from the reaction of $Pt(COD)_2$ with $Fe(CO)_5$, Scheme 1.[8] We have also prepared the mixed metal cluster complex $Ru_4Pt_2(CO)_{18}$, **11**, from the reaction of $Pt(COD)_2$ with $Ru(CO)_5$.[9] This complex has recently been used to prepare γ-Al_2O_3-supported clusters.[10]

* Corresponding author. E-mail: Adams@mail.chem.sc.edu.

(1) (a) Jia, J.; Shen, J.; Lin, L.; Xu, Z.; Zhang, T.; Liang, D. *J. Catal.* **1999**, *138*, 177. (b) Sinfelt, J. H. *Bimetallic Catalysts: Discoveries, Concepts and Applications*; Wiley: New York, 1983. (c) Sinfelt, J. H. *Bifunctional Catalysis: Adv. Chem. Eng.* **1964**, *5*, 37. (d) Sinfelt, J. H. *Sci. Am.* **1985**, *253*, 90.

(2) (a) Thomas, J. M.; Johnson, B. F. G.; Raja, R.; Sankar, G.; Midgley, P. A. *Acc. Chem. Res.* **2003**, *36*, 20. (b) Raja, R.; Khimyak, T.; Thomas, J. M.; Hermans, S.; Johnson, B. F. G. *Angew. Chem., Int. Ed.* **2001**, *40*, 4638. (c) Johnson, B. F. G. *Coord. Chem. Rev.* **1999**, *190*, 1269. (c) Hermans, S.; Raja, R.; Thomas, J. M.; Johnson, B. F. G.; Sankar, G.; Gleeson, D. *Angew. Chem., Int. Ed.* **2001**, *40*, 1211. (c) Nashner, M. S.; Frenkel, A. I.; Somerville, D.; Hills, C. W.; Shapley, J. R.; Nuzzo, R. G. *J. Am. Chem. Soc.* **1998**, *120*, 8093. (d) Hills, C. W.; Nashner, M. S.; Frenkel, A. I.; Shapley, J. R.; Nuzzo, R. G. *Langmuir* **1999**, *15*, 690.

(3) (a) Raja, R.; Sankar, G.; Hermans, S.; Shephard, D. S.; Bromley, S.; Thomas, J. M.; Johnson, B. F. G. *Chem. Commun.* **1999**, 1571. (b) Alexeev, O. S.; Gates, B. C. *Ind. Eng. Chem. Res.* **2003**, *42*, 1571.

(4) (a) Adams, R. D. In *Comprehensive Organometallic Chemistry II*; Abel, E. W., Stone, F. G. A., Wilkinson, G., Eds.; Pergamon: Oxford, 1995; Vol. 10, p 1. (b) Adams, R. D. In *The Chemistry of Metal Cluster Complexes*; Shriver, H. D., Kaesz, H. D., Adams, R. D., Eds.; VCH: New York, 1990; Chapter 3, p 121. (c) Roberts, D. A.; Geoffroy, G. L. In *Comprehensive Organometallic Chemistry II*; Wilkinson, G., Stone, F. G. A., Abel, E. W., Eds.; Pergamon: Oxford, 1995; Vol. 6, Chapter 40, p 763.

(5) Adams, R. D.; Captain, B.; Fu, W.; Smith, M. D. *J. Am. Chem Soc.* **2002**, *124*, 5628.

(6) Adams, R. D.; Captain, B.; Fu, W.; Pellechia, P. J.; Smith, M. D. *Inorg. Chem.* **2003**, *42*, 2094.

(7) Adams, R. D.; Captain, B.; Fu, W.; Smith, M. D. *J. Organomet. Chem* **2003**, *682*, 113.

(8) Adams, R. D.; Arafa, I.; Chen, G.; Lii, J. C.; Wang, J. G. *Organometallics* **1990**, *9*, 2350.

10.1021/om0342659 CCC: $27.50
Publication on Web 01/07/2004

Chart 1

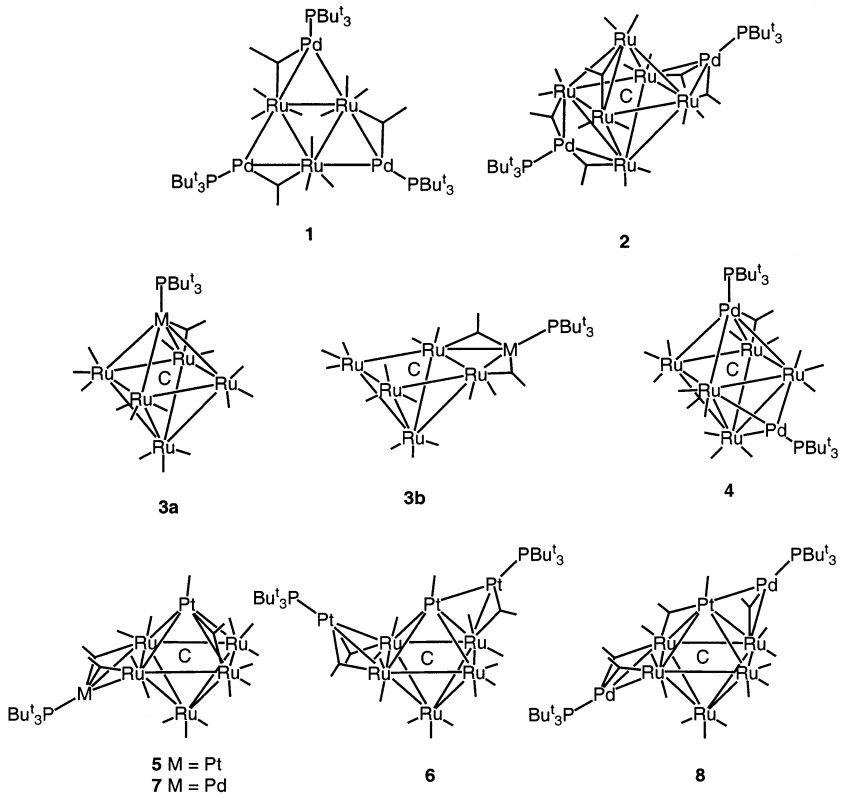

Scheme 1

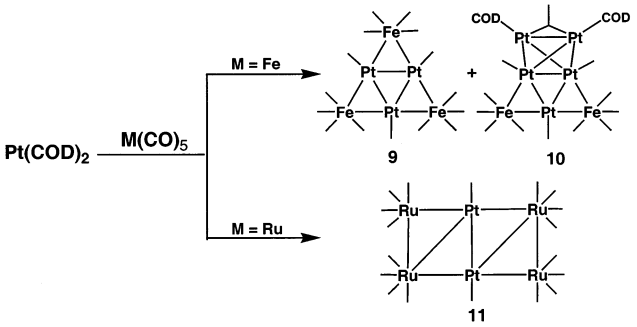

In this report, the results of our investigation of the reactions of $Pt(PBu^t_3)_2$ and $Pd(PBu^t_3)_2$ with **9** and **11** are described. Two series of structurally similar new compounds $Pt_3Fe_3(CO)_{15}[M(PBu^t_3)]$ (M = Pt, **12**; M = Pd, **14**) and $Pt_3Fe_2(CO)_{12}[M(PBu^t_3)]_2$ (M = Pt, **13**; M = Pd, **15**) as well as the new compound $Pt_2Ru_4(CO)_{17}[Pt(PBu^t_3)]$, **16**, have been isolated and structurally characterized.

Experimental Section

General Data. All reactions were performed under a nitrogen atmosphere. Reagent grade solvents were dried by the standard procedures and were freshly distilled prior to use. Infrared spectra were recorded on a Thermo-Nicolet Avatar FTIR spectrophotometer. ^{1}H NMR and ^{31}P NMR were recorded on a Varian Inova 400 spectrometer operating at 399 and 162 MHz, respectively. ^{31}P NMR spectra were externally referenced against 85% *ortho*-H_3PO_4. Elemental analyses were performed by Desert Analytics (Tucson, AZ). Product separations were performed by TLC in air on Analtech 0.25 and 0.5 mm silica gel 60 Å F_{254} glass plates. Bis(tri-*tert*-butylphosphine)platinum-(0), $Pt(PBu^t_3)_2$, and bis(tri-*tert*-butylphosphine)palladium(0), $Pd(PBu^t_3)_2$, were obtained from Strem and were used without further purification. $Pt_3Fe_3(CO)_{15}$, **9**, and $Pt_5Fe_2(CO)_{12}(COD)_2$, **10**,[8] as well as $Pt_2Ru_4(CO)_{18}$, **11**,[9] were prepared by previously reported procedures.

Reaction of 9 with $Pt(PBu^t_3)_2$. $Pt(PBu^t_3)_2$ (15.3 mg, 0.026 mmol) was added to a solution of **9** (20.0 mg, 0.017 mmol) in 20 mL of CH_2Cl_2. The reaction mixture was then stirred at room temperature for 30 min. The solvent was then removed in vacuo. The product was separated by TLC using a 2:1 hexane/methylene chloride solvent mixture to yield in order of elution 8.8 mg (33%) of $Pt_3Fe_3(CO)_{15}[Pt(PBu^t_3)]$, **12**, and 8.5 mg (27%) of $Pt_3Fe_2(CO)_{12}[Pt(PBu^t_3)]_2$, **13**. Spectral data for **12**: IR ν_{CO} (cm^{-1} in hexane): 2085 (w), 2054 (m), 2047 (vs), 2026 (m), 2009 (w), 1997 (sh), 1786 (w). ^{1}H NMR (CD_2Cl_2 in ppm): δ 1.47 (d, 27H, CH_3, $^3J_{P-H}$ = 14.3 Hz). ^{31}P{^{1}H} NMR (CD_2Cl_2 in ppm): δ 104.73 (s, 1P, $^1J_{Pt-P}$ = 6243 Hz, $^2J_{Pt-P}$ = 209 Hz). Spectral data for **13**: IR ν_{CO} (cm^{-1} in hexane): 2064 (s), 2026 (vs), 2009 (m), 1970 (w), 1957 (sh), 1776 (w). ^{1}H NMR (CD_2Cl_2 in ppm): δ 1.46 (d, 54H, CH_3, $^3J_{P-H}$ = 13.4 Hz). ^{31}P-{^{1}H} NMR (CD_2Cl_2 in ppm): δ 108.03 (s, 2P, $^1J_{Pt-P}$ = 5004 Hz, $^2J_{Pt-P}$ = 281 Hz). Anal. Calcd: 23.65 C, 2.98 H. Found: 23.34 C, 3.20 H.

Improved Yield of 13. $Pt(PBu^t_3)_2$ (21.0 mg, 0.035 mmol) was added to a solution of **9** (13.6 mg, 0.012 mmol) in 20 mL of CH_2Cl_2. The reaction mixture was then stirred at room temperature for 30 min, after which the solvent was removed in vacuo. The product was separated by TLC using a 2:1 hexane/methylene chloride solvent mixture to yield 9.5 mg (51%) of $Pt_3Fe_2(CO)_{12}[Pt(PBu^t_3)]_2$, **13**.

Conversion of 10 to 13. PBu^t_3 (6.3 mg, 0.031 mmol) was added to a solution of **10** (25.5 mg, 0.016 mmol) in 20 mL of CH_2Cl_2. The reaction mixture was then stirred at room temperature for 30 min, after which the solvent was removed in vacuo. The product was separated by TLC using a 2:1 hexane/methylene chloride solvent mixture to yield 20.3 mg (90%) of **13**.

(9) Adams, R. D.; Chen, G.; Wu, W. *J. Cluster Sci.* **1993**, *4*, 119.
(10) Alexeev, O. S.; Graham, G. W.; Shelef, M.; Adams, R. D.; Gates, B. C. *J. Phys. Chem. B* **2002**, *106*, 4697.

Conversion of 12 to 13. $Pt(PBu^t_3)_2$ (3.0 mg, 0.005 mmol) was added to a solution of **12** (8.0 mg, 0.005 mmol) in 20 mL of CH_2Cl_2. The reaction mixture was then stirred at room temperature for 30 min, after which the solvent was removed in vacuo. The product was separated by TLC using a 2:1 hexane/methylene chloride solvent mixture to yield 4.0 mg (44%) of **11** along with 2.2 mg of unreacted starting material, **12**.

Reaction of 9 with $Pd(PBu^t_3)_2$. $Pd(PBu^t_3)_2$ (27 mg, 0.053 mmol) was added to a solution of **9** (20.5 mg, 0.018 mmol) in 20 mL of CH_2Cl_2. The reaction mixture was then stirred at room temperature for 30 min, after which the solvent was removed in vacuo. The product was separated by TLC using a 2:1 hexane/methylene chloride solvent mixture to yield in order of elution 11.8 mg (54%) of $Pt_3Fe_3(CO)_{15}[Pd(PBu^t_3)]$, **14**, and 8.0 mg (28%) of $Pt_3Fe_2(CO)_{12}[Pd(PBu^t_3)]_2$, **15**. Spectral data for **14**: IR ν_{CO} (cm^{-1} in hexane): 2086 (w), 2070 (m), 2026 (vs), 2000 (m), 1989 (w), 1970 (m), 1961 (sh), 1798 (w). ^1H NMR (CD_2Cl_2 in ppm): δ 1.44 (d, 27H, CH_3, $^3J_{P-H} = 11.5$ Hz). $^{31}P\{^1H\}$ NMR (CD_2Cl_2 in ppm): δ 79.64 (s, 1P, $^2J_{Pt-P} = 140$ Hz). Spectral data for **15**: IR ν_{CO} (cm^{-1} in hexane): 2065 (s), 2026 (vs), 2008 (m), 1971 (w), 1962 (sh), 1823 (w). ^1H NMR (CD_2Cl_2 in ppm): δ 1.42 (d, 54H, CH_3, $^3J_{P-H} = 12.6$ Hz). $^{31}P\{^1H\}$ NMR (CD_2Cl_2 in ppm): δ 97.64 (s, 2P, $^2J_{Pt-P} = 132$ Hz). Anal. Calcd: 26.19 C, 3.30 H. Found: 26.28 C, 3.28 H.

Reaction of 11 with $Pt(PBu^t_3)_2$. $Pt(PBu^t_3)_2$ (7.4 mg, 0.012 mmol) was added to a solution of **11** (14.0 mg, 0.012 mmol) in 20 mL of CH_2Cl_2. The reaction mixture was then stirred at room temperature for 30 min, after which the solvent was removed in vacuo. The products were separated by TLC using a 3:1 hexane/methylene chloride solvent mixture to yield 13.5 mg (75%) of $Pt_2Ru_4(CO)_{17}[Pt(PBu^t_3)]$, **16**. Spectral data for **16**: IR ν_{CO} (cm^{-1} in hexane): 2101 (m), 2063 (vs), 2056 (m), 2039 (s), 2033 (m), 2025 (m), 2003 (m), 1990 (m), 1825 (w). ^1H NMR (CD_2Cl_2 in ppm): δ 1.45 (d, 27H, CH_3, $^3J_{P-H} = 13.3$ Hz). $^{31}P\{^1H\}$ NMR (CD_2Cl_2 in ppm): δ 113.82 (s, 1P, $^1J_{Pt-P} = 5277$ Hz, $^2J_{Pt-P} = 355$ Hz, $^2J_{Pt-P} = 163$ Hz). Anal. Calcd: 20.87 C, 1.62 H. Found: 20.63 C, 1.82 H.

Crystallographic Analyses. Dark brown crystals of **12**, **13**, and **14**; dark green crystals of **15**; and dark red crystals of **16** suitable for diffraction analysis were grown by slow evaporation of solvent from solutions of the pure compound in hexane/methylene chloride solvent mixtures at 5 °C. Each data crystal was glued onto the end of a thin glass fiber. X-ray intensity data were measured using a Bruker SMART APEX CCD-based diffractometer using Mo Kα radiation ($\lambda = 0.71073$ Å). The raw data frames were integrated with the SAINT+ program using a narrow-frame integration algorithm.[11] Corrections for the Lorentz and polarization effects were also applied by using the program SAINT. An empirical absorption correction based on the multiple measurement of equivalent reflections was applied by using the program SADABS. All structures were solved by a combination of direct methods and difference Fourier syntheses and refined by full-matrix least squares on F^2, by using the SHELXTL software package.[12] All non-hydrogen atoms were refined with anisotropic displacement parameters. Hydrogen atoms were placed in geometrically idealized positions and refined as standard riding atoms. Crystal data, data collection parameters, and results of the analyses for compounds **12** and **13** are given in Table 1 and for compounds **14**, **15**, and **16** are given in Table 2.

Compounds **12** and **14** are isomorphous and isostructural and crystallized in the monoclinic crystal system. The two possible space groups $P2_1$ and $P2_1/m$ were identified on the basis of the systematic absences in the intensity data. The latter space group was chosen and confirmed by the successful solution and refinement of the structures. In compound **12**, atom C(40) and, in compound **14**, atom C(50) were both refined with an isotropic displacement parameter because they gave a negative thermal parameter when refined anisotropically. Compound **13** also crystallized in the monoclinic crystal system, and the space group $P2_1/c$ was identified uniquely on the basis of the systematic absences in the intensity data.

Compounds **15** and **16** both crystallized in the triclinic crystal system. For both compounds the space group $P\bar{1}$ was assumed and confirmed by the successful solution and refinement of the structure. For the structures of **12**−**15** one molecule of CH_2Cl_2 from the crystallization solvent was found cocrystallized with the complex. The CH_2Cl_2 molecules were located and refined successfuly with isotropic displacement parameters.

Table 1. Crystallographic Data for Compounds 12 and 13

	12	**13**
empirical formula	$Pt_4Fe_3PO_{15}C_{27}H_{27}\cdot CH_2Cl_2$	$Pt_5Fe_2P_2O_{12}C_{36}H_{54}\cdot CH_2Cl_2$
fw	1655.29	1912.81
cryst syst	monoclinic	monoclinic
lattice params		
a (Å)	10.1914(13)	13.9156(8)
b (Å)	17.009(2)	18.2636(11)
c (Å)	12.7509(16)	21.2496(13)
α (deg)	90	90
β (deg)	108.839(2)	101.737(1)
γ (deg)	90	90
V (Å^3)	2091.9(5)	5287.6(5)
space group	$P2_1/m$	$P2_1/c$
Z-value	2	4
ρ_{calc} (g cm^{-3})	2.628	2.403
μ(Mo Kα) (mm^{-1})	14.558	13.92
temperature (K)	296	296
$2\theta_{max}$ (deg)	56.92	50.06
no. of observations	4373	7959
no. of params	276	544
goodness of fit	1.046	1.040
max. shift in cycle	0.001	0.001
residuals: R_1; wR_2 ($I > 2\sigma(I)$)[a]	0.0552; 0.1421	0.0551; 0.1330
abs corr	SADABS	SADABS
max./min.	1.000/0.266	1.000/0.296
largest peak in final diff map (e Å^{-3})	5.953	2.784

[a] $R = \sum_{hkl}(||F_{obs}| - |F_{calc}||)/\sum_{hkl}|F_{obs}|$; $R_w = [\sum_{hkl}w(|F_{obs}| - |F_{calc}|)^2/\sum_{hkl}wF^2_{obs}]^{1/2}$; $w = 1/\sigma^2(F_{obs})$; GOF $= [\sum_{hkl}w(|F_{obs}| - |F_{calc}|)^2/(n_{data} - n_{vari})]^{1/2}$.

Results

The reaction of **9** with $Pt(PBu^t_3)_2$ at room temperature afforded two new complexes, $Pt_3Fe_3(CO)_{15}[Pt(PBu^t_3)]$, **12**, in 33% yield and $Pt_3Fe_2(CO)_{12}[Pt(PBu^t_3)]_2$, **13** in 27% yield, eq 1. The yield of compound **13** was increased to

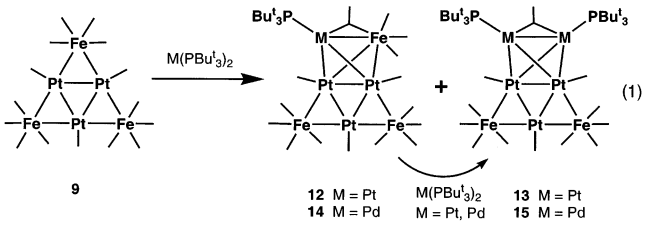

(1)

51% when the amount of $Pt(PBu^t_3)_2$ was increased to 3 times the amount of **9** in the reaction mixture. This reaction was followed by ^{31}P NMR, which showed the formation of $Pt_3(CO)_3(PBu^t_3)_3$[13] as a major side product and of $Fe(CO)_4(PBu^t_3)$[14] as a minor product. Compounds

(11) *SAINT+, version 6.02a*; Bruker Analytical X-ray Systems, Inc.: Madison, WI, 1998.
(12) Sheldrick, G. M. *SHELXTL, version 5.1*; Bruker Analytical X-ray Systems, Inc.: Madison, WI, 1997.

Table 2. Crystallographic Data for Compounds 14, 15, and 16

	14	15	16
empirical formula	$Pt_3PdFe_3PO_{15}C_{27}H_{27}\cdot CH_2Cl_2$	$Pt_3Pd_2Fe_2P_2O_{12}C_{36}H_{54}\cdot CH_2Cl_2$	$Pt_3Ru_4PO_{17}C_{29}H_{27}$
fw	1566.60	1735.43	1668.03
cryst syst	monoclinic	triclinic	triclinic
lattice params			
a (Å)	10.0725(6)	13.0758(11)	10.4091(5)
b (Å)	16.8032(10)	13.1261(11)	11.4151(5)
c (Å)	12.7612(8)	17.1019(14)	19.0923(9)
α (deg)	90	103.478(2)	97.7180(10)
β (deg)	108.8950(10)	98.332(2)	96.1070(10)
γ (deg)	90	99.854(2)	111.6970(10)
V (Å^3)	2043.4(2)	2759.5(4)	2058.53(17)
space group	$P2_1/m$	$P\bar{1}$	$P\bar{1}$
Z-value	2	2	2
ρ_{calc} (g cm^{-3})	2.546	2.089	2.691
μ(Mo Kα) (mm^{-1})	11.923	8.924	11.685
temperature (K)	150	296	293
$2\theta_{max}$ (deg)	50.06	56.64	52.04
no. of observations	3445	10946	7255
no. of params	279	544	496
goodness of fit	1.271	1.012	1.019
max. shift in cycle	0.001	0.001	0.000
Residuals: R_1; wR_2 ($I > 2\sigma(I)$)[a]	0.0413: 0.0975	0.0384: 0.1019	0.0229; 0.0498
abs corr	SADABS	SADABS	SADABS
max./min.	1.000/0.598	1.000/0.451	1.000/0.726
largest peak in final diff map (e Å^{-3})	2.297	2.839	1.433

[a] $R = \sum_{hkl}(||F_{obs}| - |F_{calc}||)/\sum_{hkl}|F_{obs}|$; $R_w = [\sum_{hkl}w(|F_{obs}| - |F_{calc}|)^2/\sum_{hkl}wF^2_{obs}]^{1/2}$; $w = 1/\sigma^2(F_{obs})$; GOF $= [\sum_{hkl}w(|F_{obs}| - |F_{calc}|)^2/(n_{data} - n_{vari})]^{1/2}$.

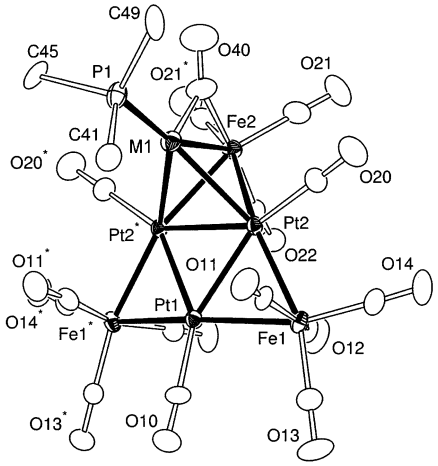

Figure 1. ORTEP diagram of the molecular structure of $Pt_3Fe_3(CO)_{15}[M(PBu^t_3)]$ (M1 = Pt(4), **12**; M1 = Pd(1), **14**) showing 40% thermal ellipsoid probabilities. Methyl groups have been omitted for clarity.

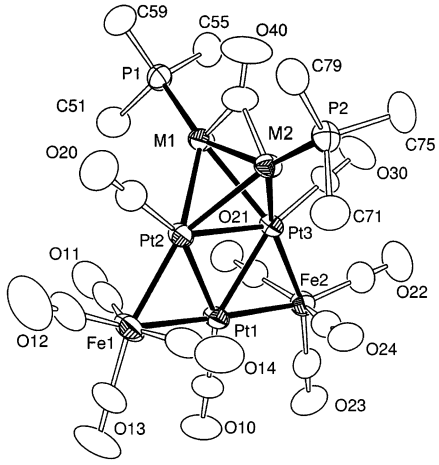

Figure 2. ORTEP diagram of the molecular structure of $Pt_3Fe_2(CO)_{12}[M(PBu^t_3)]_2$ (M1 = Pt(4) and M2 = Pt(5), **13**; M1 = Pd(1) and M2 = Pd(2), **15**) showing 40% thermal ellipsoid probabilities. Methyl groups have been omitted for clarity.

12 and **13** were characterized by IR, ^{1}H and ^{31}P NMR, and single-crystal X-ray diffraction analyses. ORTEP diagrams of the molecular structures of **12** and **13** are shown in Figures 1 and 2, respectively. Selected intramolecular distances and angles for compounds **12** and **13** are listed in Tables 3 and 4, respectively. Compound **12** contains a crystallographically imposed plane of symmetry that passes through the metal atoms Pt(1), M(1), and Fe(2) and the bridging carbonyl ligand. The methyl groups on the phosphine ligand are disordered between two positions. Only one of the disordered orientations is shown in Figure 1. Compound **12** can be viewed as a simple adduct of **9** because no carbonyl ligands were eliminated from **9** during the course of the reaction. The structure of **12** contains a $Pt(PBu^t_3)$ group bridging one of the three Pt_2Fe triangular groups of the starting compound **9**. The presence of the $Pt(PBu^t_3)$ group causes significant increases in the metal−metal bond lengths in the Fe(2)−Pt(2)−Pt(2)* triangle to which the $Pt(PBu^t_3)$ group is added relative to that in **12**: 2.580(2) and 2.587 Å for Pt−Fe and Pt−Pt, respectively, in **9** versus 2.742(2) and 2.7830(6) Å in **12**. The iron atoms are displaced out of the plane of the central Pt_3 triangle on the same side by 0.43 Å for Fe(1) and Fe(1)* and 0.70 Å for Fe(2).

The structure of **13** is similar to that of the known compound **10** and consists of a tetrahedron of four platinum atoms and a fifth Pt(1) that bridges an edge of this Pt_4 cluster. There are also two $Fe(CO)_4$ groups that bridge the edges between Pt(1) and the tetrahedron. The bond between Pt(4) and Pt(5) is bridged by a carbonyl ligand, and both platinum atoms contain one

(13) Goel, R. G.; Ogini, W. O.; Srivastava, R. C. *J. Organomet. Chem.* **1981**, *214*, 405.
(14) Schumann, H.; Opitz, J. *J. Organomet. Chem.* **1979**, *166*, 233.

Table 3. Selected Intramolecular Distances and Angles for Compounds 12 and 14[a]

compound **12**		compound **14**	
atoms	distance (Å)	atoms	distance (Å)
Pt(1)−Fe(1)	2.5939(15)	Pt(1)−Fe(1)	2.5898(14)
Pt(1)−Pt(2)	2.6056(7)	Pt(1)−Pt(2)	2.6053(6)
Pt(2)−Fe(1)	2.5679(16)	Pt(2)−Fe(1)	2.5719(14)
Pt(2)−Fe(2)	2.624(2)	Pt(2)−Fe(2)	2.6248(18)
Pt(2)−Pt(2)*	2.6240(8)	Pt(2)−Pt(2)*	2.6175(7)
Pt(2)−Pt(3)	2.7830(6)	Pt(2)−Pd(1)	2.7861(10)
Pt(3)−Fe(2)	2.742(2)	Pd(1)−Fe(2)	2.743(2)
Pt(3)−P(1)	2.293(4)	Pd(1)−P(1)	2.357(4)
C−O (av)	1.127	C−O (av)	1.132
atoms	angle (deg)	atoms	angle (deg)
Pt(1)−Pt(2)−Fe(2)	117.39(3)	Pt(1)−Pt(2)−Fe(2)	117.73(3)
Pt(1)−Pt(2)−Pt(3)	102.888(19)	Pt(1)−Pt(2)−Pd(1)	102.63(2)
Pt(2)−Pt(3)−Pt(2)*	56.255(19)	Pt(2)−Pd(1)−Pt(2)*	56.04(3)
Pt(2)−Fe(1)−Pt(1)	60.63(3)	Pt(2)−Fe(1)−Pt(1)	60.63(3)
Pt(2)−Fe(2)−Pt(3)	62.43(5)	Pt(2)−Fe(2)−Pd(1)	62.49(5)
Fe(1)−Pt(1)−Pt(2)	59.19(4)	Fe(1)−Pt(1)−Pt(2)	59.35(3)
Fe(1)−Pt(2)−Pt(1)	60.18(4)	Fe(1)−Pt(2)−Pt(1)	60.03(3)
Fe(1)−Pt(2)−Fe(2)	154.70(6)	Fe(1)−Pt(2)−Fe(2)	155.62(5)
Fe(1)−Pt(2)−Pt(3)	143.58(4)	Fe(1)−Pt(2)−Pd(1)	142.72(4)
Fe(2)−Pt(2)−Pt(3)	60.86(4)	Fe(2)−Pt(2)−Pd(1)	60.84(5)
Fe(2)−Pt(3)−Pt(2)	56.71(4)	Fe(2)−Pd(1)−Pt(2)	56.67(4)
P(1)−Pt(3)−Fe(2)	159.65(14)	P(1)−Pd(1)−Fe(2)	158.73(13)
P(1)−Pt(3)−Pt(2)	139.00(9)	P(1)−Pd(1)−Pt(2)	139.70(8)
Pt−C−O (av)	177.1	Pt−C−O (av)	177.3
Fe−C−O (av)	176.1	Fe−C−O (av)	176.1

[a] Estimated SDs in the least significant figure are given in parentheses.

Table 4. Selected Intramolecular Distances and Angles for Compounds 13 and 15[a]

compound **13**		compound **15**	
atoms	distance (Å)	atoms	distance (Å)
Pt(1)−Fe(1)	2.5919(17)	Pt(1)−Fe(2)	2.5954(11)
Pt(1)−Fe(2)	2.5957(17)	Pt(1)−Fe(1)	2.5978(9)
Pt(1)−Pt(2)	2.6777(7)	Pt(1)−Pt(2)	2.6582(3)
Pt(1)−Pt(3)	2.6827(6)	Pt(1)−Pt(3)	2.6502(4)
Pt(2)−Fe(1)	2.5379(17)	Pt(2)−Fe(1)	2.5263(9)
Pt(2)−Pt(3)	2.6917(6)	Pt(2)−Pt(3)	2.6757(4)
Pt(2)−Pt(4)	2.7638(6)	Pt(2)−Pd(1)	2.7409(6)
Pt(2)−Pt(5)	2.7469(6)	Pt(2)−Pd(2)	2.7319(5)
Pt(3)−Fe(2)	2.5488(18)	Pt(3)−Fe(2)	2.5362(10)
Pt(3)−Pt(4)	2.7619(6)	Pt(3)−Pd(1)	2.7404(5)
Pt(3)−Pt(5)	2.7605(6)	Pt(3)−Pd(2)	2.7521(5)
Pt(4)−Pt(5)	2.7545(6)	Pd(1)−Pd(2)	2.7778(7)
Pt(4)−P(1)	2.300(3)	Pd(1)−P(1)	2.3536(18)
Pt(5)−P(2)	2.294(3)	Pd(2)−P(2)	2.3502(17)
C−O (av)	1.138	C−O (av)	1.129
atoms	angle (deg)	atoms	angle (deg)
Pt(1)−Pt(2)−Pt(5)	111.88(2)	Pt(1)−Pt(2)−Pd(2)	113.222(15)
Pt(1)−Pt(3)−Pt(5)	111.302(19)	Pt(1)−Pt(3)−Pd(1)	110.171(15)
Pt(4)−Pt(3)−Pt(5)	59.840(15)	Pd(1)−Pt(3)−Pd(2)	60.763(15)
Fe(2)−Pt(3)−Pt(4)	149.26(5)	Fe(2)−Pt(3)−Pd(1)	148.64(3)
Fe(2)−Pt(3)−Pt(5)	150.08(5)	Fe(2)−Pt(3)−Pd(2)	149.90(3)
P(1)−Pt(4)−Pt(3)	142.01(8)	P(1)−Pd(1)−Pt(2)	142.41(5)
P(1)−Pt(4)−Pt(5)	152.07(8)	P(1)−Pd(1)−Pt(3)	141.98(5)
Pt−C−O (av)	178.1	Pt−C−O (av)	178.9
Fe−C−O (av)	176.8	Fe−C−O (av)	176.5

[a] Estimated SDs in the least significant figure are given in parentheses.

PBu^t_3 ligand. The Pt−Pt bonds of the tetrahedron, especially the Pt(4)−Pt(5) bond, are significantly shorter in **13** (Pt(4)−Pt(5) = 2.7545 Å) than in **10** (Pt(4)−Pt(5) = 2.958 Å).[8] According to the methodology developed by Mingos,[15] the number of valence electrons in the Pt_5Fe_2 cluster of this geometry should be 98; however the total valence electron count of **13** is only 94. Thus,

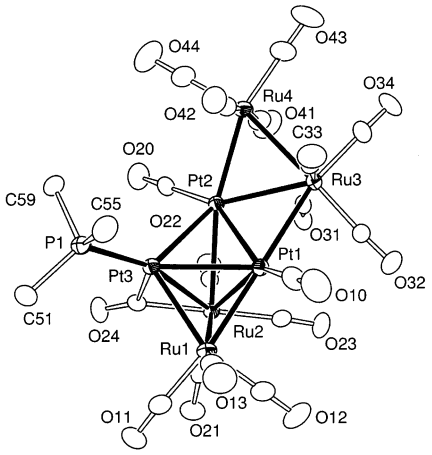

Figure 3. ORTEP diagram showing the molecular structure of $Pt_2Ru_4(CO)_{17}[Pt(PBu^t_3)]$, **16**, showing 40% thermal ellipsoid probabilities. Methyl groups have been omitted for clarity.

Table 5. Selected Intramolecular Distances and Angles for Compound 16[a]

atoms	distance (Å)	atoms	angle (deg)
Pt(1)−Pt(2)	2.6753(3)	Pt(1)−Pt(2)−Ru(3)	64.034(9)
Pt(1)−Pt(3)	2.8737(3)	Pt(1)−Pt(2)−Pt(3)	63.163(7)
Pt(1)−Ru(1)	2.6228(4)	Pt(2)−Ru(3)−Pt(1)	56.026(8)
Pt(1)−Ru(2)	2.8234(4)	Pt(2)−Ru(4)−Ru(3)	60.523(11)
Pt(1)−Ru(3)	2.9004(4)	Pt(3)−Pt(1)−Ru(3)	118.148(10)
Pt(2)−Pt(3)	2.8077(3)	Ru(1)−Pt(1)−Pt(2)	113.667(11)
Pt(2)−Ru(2)	2.9959(4)	Ru(1)−Pt(3)−Pt(1)	55.846(9)
Pt(2)−Ru(3)	2.7921(4)	Ru(1)−Pt(3)−Pt(2)	106.711(11)
Pt(2)−Ru(4)	2.6888(4)	Ru(4)−Ru(3)−Pt(1)	107.552(15)
Pt(3)−Ru(1)	2.7195(4)	Ru(4)−Pt(2)−Ru(2)	164.085(13)
Pt(3)−Ru(2)	2.7977(4)	P(1)−Pt(3)−Ru(2)	162.97(3)
Ru(1)−Ru(2)	2.7709(5)	P(1)−Pt(3)−Pt(2)	128.58(3)
Ru(3)−Ru(4)	2.8452(5)	Pt−C−O (av)	177.3
C−O (av)	1.136	Ru−C−O (av)	175.8

[a] Estimated SDs in the least significant figure are given in parentheses.

13 is four electrons deficient. This deficiency could lead to some partial multiple bonding character between the metal atoms and could explain the relative shortness of the Pt−Pt bonds in **13**. Compound **12** can be converted to **13** in 44% yield by reaction with an excess of $Pt(PBu^t_3)_2$ (eq 1), but an even more convenient route to **13** is by a simple substitution of the COD groups on **10** by PBu^t_3, which gives **13** (90% yield).

The reaction of **9** with $Pd(PBu^t_3)_2$ yields the monopalladium and dipalladium complexes $Pt_3Fe_3(CO)_{15}[Pd(PBu^t_3)]$, **14**, and $Pt_3Fe_3(CO)_{12}[Pd(PBu^t_3)]_2$, **15**, in 54% and 28% yields, respectively. Both products were characterized by IR, ^1H and ^{31}P NMR, and single-crystal X-ray diffraction analyses. ORTEP diagrams of the molecular structures of **14** and **15**, M = Pd, are also represented in Figures 1 and 2, respectively. Selected intramolecular distances and angles for compounds **14** and **15** are listed in Tables 3 and 4, respectively. Compounds **14** and **15** are isostructural to the platinum homologues **12** and **13**. Bond distances and angles for **14** and **15** are very similar to those of **12** and **13**, respectively.

The reaction of **11** with $Pt(PBu^t_3)_2$ at room temperature afforded the new complex $Pt_2Ru_4(CO)_{17}[Pt(PBu^t_3)]$,

(15) Mingos, D. M. P.; Evans, D. G. *J. Organomet. Chem.* **1983**, *251*, C13.

16, in 75% yield. The product was characterized by IR, ^{1}H and ^{31}P NMR, and single-crystal X-ray diffraction analyses. An ORTEP diagram of the molecular structure of **16** is shown in Figure 3. Selected intramolecular bond distances and bond angles are listed in Table 5. The structure of **16** was derived from that of **11** by the addition of a Pt(PBu$^t_3$) group across the butterfly arrangement of the four metal atoms Ru(1), Ru(2), Pt(1), and Pt(2); see Figure 3 and eq 2. There is a bridging carbonyl ligand across the Ru(2)−Pt(3) bond. The bond distances of **16** are very similar to the parent compound **11**. Unlike the M(PBu$^t_3$) addition reactions to **9**, this reaction involved the loss of one CO ligand from the parent complex **11**. Compound **11** also reacts with Pd(PBu$^t_3$)$_2$; however this product was not sufficiently stable to be isolated and characterized.

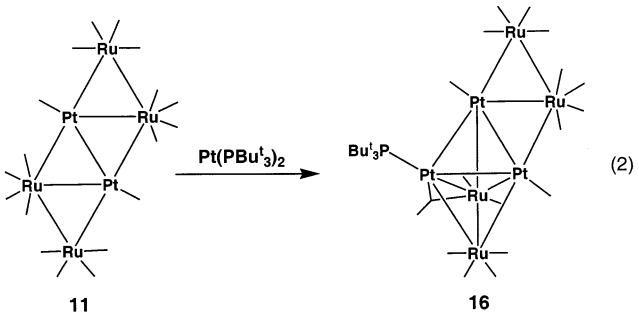

(2)

Acknowledgment. This research was supported by the Office of Basic Energy Sciences of the U.S. Department of Energy under Grant No. DE-FG02-00ER14980. We thank Strem for the generous donation of a sample of Pt(PBu$^t_3$)$_2$.

Supporting Information Available: CIF tables for the structural analyses of **12**−**16**. This material is available free of charge via the Internet at http://pubs.acs.org.

OM0342659